HHS Public Access

Author manuscript

Osteoarthritis Cartilage. Author manuscript; available in PMC 2022 March 01.

Published in final edited form as:

Osteoarthritis Cartilage. 2021 March ; 29(3): 402–412. doi:10.1016/j.joca.2020.11.004.

The combination of mitogenic stimulation and DNA damage induces chondrocyte senescence

Michaela E. Copp[1,2,4], **Margaret C. Flanders**[2,3,4], **Rachel Gagliardi**[3,4], **Jessica M. Gilbertie**[3,4], **Garrett A. Sessions**[2], **Susanna Chubinskaya**[5], **Richard F. Loeser**[2,6], **Lauren V. Schnabel**[2,3,4], **Brian O. Diekman**[*,1,2,4]

[1]Joint Department of Biomedical Engineering, University of North Carolina at Chapel Hill, Chapel Hill, NC, USA and North Carolina State University, Raleigh, NC, USA

[2]Thurston Arthritis Research Center, The University of North Carolina at Chapel Hill, Chapel Hill, NC, USA

[3]NC State College of Veterinary Medicine, North Carolina State University, Raleigh, NC, USA

[4]Comparative Medicine Institute, North Carolina State University, Raleigh, NC, USA

[5]Department of Pediatrics, Rush University Medical Center, Chicago, IL, USA

[6]Division of Rheumatology, Allergy, and Immunology, University of North Carolina, Chapel Hill, NC, USA

Abstract

Objective: Cellular senescence is a phenotypic state characterized by stable cell-cycle arrest, enhanced lysosomal activity, and the secretion of inflammatory molecules and matrix degrading enzymes. Senescence has been implicated in osteoarthritis (OA) pathophysiology; however, the mechanisms that drive senescence induction in cartilage and other joint tissues are unknown. While numerous physiological signals are capable of initiating senescence, one emerging theme is that damaged cells convert to senescence in response to sustained mitogenic stimulation. The goal of this study was to develop an *in vitro* articular cartilage explant model to investigate the mechanisms of senescence induction.

Design: This study utilized healthy cartilage derived from cadaveric equine stifles and human ankles. Explants were irradiated to initiate DNA damage, and mitogenic stimulation was provided

[*]**Corresponding Author:** Brian Diekman, Thurston Arthritis Research Center, The University of North Carolina School of Medicine 3300 Thurston Building, Campus Box #7280, Chapel Hill, NC 27599-7280, Phone: (919) 445 - 2613, Fax: (919) 966 - 1739, bdiekman@email.unc.edu.

Contributions:

The conception and design of this study was done by MEC and BOD. Collection and analysis of data conducted by MEC, MCF, GAS and BOD. Study materials provided by RG, JMG, RFL, LVS, and SC. MEC drafted the article and RFL, LVS, SC, and BOD contributed to the critical revision of the article. All authors have read and approved the final manuscript. BOD takes responsibility for the integrity of the work as a whole.

Competing Interest Statement:

Dr. Loeser has served as a consultant for Unity Biotechnology. The other authors declare they have no potential conflicts of interest.

through serum-containing medium and treatment with transforming growth factor β1 and basic fibroblastic growth factor. Readouts of senescence were a quantitative flow cytometry assay to detect senescence-associated β galactosidase activity (SA-β-gal), immunofluorescence for p16 and γH2AX, and qPCR for the expression of inflammatory genes.

Results: Human cartilage explants required both irradiation and mitogenic stimulation to induce senescence as compared to baseline control conditions (7.16% vs. 2.34% SA-β-gal high, p=0.0007). These conditions also resulted in chondrocyte clusters within explants, a persistent DNA damage response, increased p16, and gene expression changes.

Conclusions: Treatment of cartilage explants with mitogenic stimuli in the context of cellular damage reliably induces high levels of SA-β-gal activity and other senescence markers, which provides a physiologically relevant model system to investigate the mechanisms of senescence induction.

Keywords

SA-β-gal; DNA damage; osteoarthritis; aging; TGF-β1; bFGF

Introduction:

Osteoarthritis (OA) is a disease characterized by joint pain and progressive degradation of articular cartilage and other tissues of the joint[1, 2]. As the most common chronic disease of the articular joint, OA produces a substantial burden on society and the economy[3, 4]. Despite increasing knowledge about factors contributing to the progression of OA, there are no approved disease-modifying therapies[5], leading to high rates of total joint replacement[6]. Risk factors for OA include obesity, joint injury, and genetic predisposition, with the most dominant risk factor being aging[7, 8]. Cellular senescence has been described as a key phenotype associated with aging[9], and there is mounting evidence that the accumulation of senescent cells in the joint during both aging and in response to injury contributes to the development of OA[10–14]. Senescent chondrocytes likely contribute to tissue degradation by producing pro-inflammatory and matrix-degrading molecules known collectively as the senescence-associated secretory phenotype (SASP)[15, 16]. Significant advances have begun to unravel the role of senescence in OA and the therapeutic implications of such findings, including the potential for senolytic therapy as a potential disease-modifying therapy[13, 17]. However, there has been less progress in understanding the underlying biologic processes that drive the accumulation of senescent cells in the joint space. With clinical trials that target senescent cells in the joint underway (e.g. NCT03513016), it is imperative to identify the physiological contexts that promote senescence induction[18]. The goal of this study was to investigate the mechanisms of senescence induction in articular cartilage through the use of explants from healthy equine and human cadaveric donors.

Senescent cells display stable cell cycle arrest even in an environment that would normally promote cell division, which distinguishes the senescent phenotype from quiescence[19]. Indeed, there is evidence that a pro-growth environment - termed expansion signals to account for stimuli associated with proliferation or cellular hypertrophy - drives senescence

induction in cells harboring strong growth arrest (reviewed in [20]). The upregulation of metabolic processes associated with an ongoing stress response, combined with absence of division, result in abnormally high lysosomal activity in senescent cells. This feature has been used to identify senescence through detection of β-galactosidase activity at the sub-optimal pH of 6.0 - the senescence-associated β-galactosidase (SA-β-gal) assay[21, 22]. We recently used cartilage explants from $p16^{tdTomato}$ knock-in senescence reporter mice[23] to show that transforming growth factor beta (TGF-β1) and basic fibroblastic growth factor (bFGF), both of which are released from cartilage tissue in response to injury and degradation, were potent inducers of senescence by the measure of $p16^{Ink4a}$ promoter activity[24]. In this study, we implement a quantitative flow-cytometry-based assay of SA-β-gal activity to demonstrate that the combination of cellular damage (by irradiation) and cell-expansion stimuli (through culture with growth factors) induces a senescent phenotype.

Materials and methods:

Acquisition of equine cartilage explants

Cartilage isolation was performed under IACUC approval at the North Carolina State University College of Veterinary Medicine from donor horses that were euthanized for reasons outside of this study. Horses were between 4 and 7 years of age and included 3 geldings and 4 non-parous mares. A series of 6 mm biopsy punches were taken from the femoral trochlear ridges of thoroughbred horses without known patellofemoral disease or any macroscopic signs of cartilage damage.

Acquisition of human cartilage explants

Tali from cadaveric ankle joints were obtained from organ donors within 24 hours of death through the Gift of Hope Organ and Tissue Donor Network (Itasca, IL). A tissue repository for donor material supported by the Material Transfer Agreement has been established within the Department of Pediatrics (Dr. Chubinskaya, Director) and has been approved by the Research and Clinical Trials Administration Office at Rush University Medical Center (Chicago, IL), ORA 08082803IRB01AM2. An exemption for IRB approval was granted on February 15, 2016 according to the Deceased Subjects Rule. Samples were shipped overnight with ice packs to the University of North Carolina at Chapel Hill. Ankle tissue was used instead of knee tissue due to greater availability, but donor-matched comparisons of chondrocytes from ankle and femoral cartilage have shown a similar response to stimuli in culture[25]. Donors had no history of joint disease and ankle tissue was screened with a modified Collins grade on a 4-point scale[26]. Only ankle joints with grades of 0 – 2 (eliminating joints with evidence of erosion to the subchondral bone in any region) were used to avoid the confounding factor of extensive cartilage degeneration. Explants of 5 mm were taken from the talar surface for culture. Tissue was used from a total of 31 donors - 22 males and 9 females ranging from 38 to 73 years of age. Donor information is included in a table alongside the appropriate figures.

Explant culture for senescence induction

The experimental layout is provided as a schematic in Figure 1. Harvested equine explants were allowed to recover in 6-well plates for 3–7 days in the following control medium:

DMEM/F12 medium (11330, Thermo Fisher Scientific, Waltham, MA), 10% fetal bovine serum (Seradigm 1500–500; VWR International, West Chester, PA, USA), penicillin and streptomycin (15140; Thermo Fisher Scientific), gentamicin (15750; Thermo Fisher Scientific), and amphotericin B (A2942; MilliporeSigma, Burlington, MA, USA). Half of the explants from each horse donor were irradiated with 10 Gy using a RS2000 Biological Irradiator, with the other half remaining as experimental controls. Post irradiation, the explants were cultured in the same control medium for 7 – 10 days before digestion for monolayer culture. Human cartilage explants were cultured in the same way as with equine explants, with the exception that mitogenic stimulation was included as an additional experimental factor. Mitogenic stimulus conditions were applied immediately after irradiation and consisted of control medium with the addition of 1 ng/mL TGF-β1 and 5 ng/mL basic fibroblastic growth factor (bFGF) (PHG9204 and PHG0264; Thermo Fisher Scientific).

Monolayer culture of primary chondrocytes for maturation of senescent phenotype

Following senescence induction in explant culture, chondrocytes were isolated from cartilage by enzymatic digestion with Pronase (1 hour) and subsequently with Collagenase P (overnight) as described previously[27]. The approximate yield was 100,000 cells per 5 mm diameter × ~1.5 mm depth explant. Isolated chondrocytes were resuspended in 1 mL of media and plated in 12-well plates at a concentration of 6.4×10^4 cells per cm^2. All cells (including those from the growth factor treated explants) were cultured in control medium, with media being changed every 2–3 days. The chondrocytes were cultured in monolayer for 10 – 12 days without passaging before SA-β-Gal flow cytometry analysis. Images of chondrocytes at the end of monolayer culture were taken with an EVOS FL microscope (Life Technologies, Carlsbad, CA).

Flow cytometry analysis of SA-β-gal

SA-β-gal activity in the chondrocytes after senescence induction and monolayer culture was evaluated using the CellEvent™ Senescence Green Flow Cytometry Assay Kit (C10840; Thermo Fisher Scientific). This kit utilizes the same principle as the traditional colorimetric SA-β-gal assay in that excessive galactosidase activity is detected at the sub-optimal pH of 6.0. In this case, the CellEvent™ probe contains two galactosidase moieties and cleavage releases a fluorescent signal that is retained in the cytoplasm for detection by flow cytometry. As consistent with the manufacturer recommendations, the working solution was prepared by diluting the CellEvent™ Senescence Green Probe (1,000X) into the CellEvent™ Senescence Buffer that had been warmed to 37°C. Chondrocytes to be analyzed were washed twice with 1x PBS (14190136, Gibco), incubated at 37°C for 5 minutes in Trypsin-EDTA (T4174; Sigma-Aldrich, St. Louis, MO), and neutralized with 50 μg/mL Soybean Trypsin Inhibitor (17075029, Thermo Fisher Scientific) with EDTA (46–034-CI, Corning, Corning, NY). The mixture was centrifuged at 800 ×g for 6 minutes, washed with PBS, and fixed with 2% paraformaldehyde in PBS (1:1 volume of cells in PBS and 4% solution made from 16% stock, 43368, Alfa Aesar, Haverhill, MA) for 10 minutes at room temperature. Fixed cells were washed with 1% bovine serum albumin (A7906; Sigma Aldrich) in PBS and resuspended in 100 μL of the working solution. The chondrocytes were incubated with the dye at 37°C for 2 hours at 300 rpm in a ThermoMixer C (Eppendorf,

Hamburg, Germany). After incubation, the chondrocytes were washed with 1 mL of PBS and resuspended in 200 μL of PBS. The stained cells were filtered with a 30-μm strainer to achieve a single-cell suspension. Flow cytometry analysis was performed using an Attune NxT (Thermo Fisher Scientific) with a 488 nm laser, and analysis performed using FCS Express 8 software (De Novo Software, Glendale, CA, USA).

Immunofluorescence

After explant digestion, cells were plated into 8-well chamber slides (Nunc Lab-Tek II, Thermo Fisher Scientific 154534) at the same density as other monolayer cultures. After 12 days, cells were fixed in 1% paraformaldehyde and permeabilized with 0.25% Triton X-100 to prepare for immunofluorescence. Cells were blocked with a solution of 1% BSA, 0.1% Tween, and 22.5 mg/ml glycine and then incubated overnight at 4°C with primary antibodies (p16: CINtec®, pre-diluted, Roche Diagnostics; γH2AX: sc-517348, 1:100, Santa Cruz Biotechnology). The CINtec® p16 antibody has been extensively characterized through its approved use in the evaluation of cervical biopsy specimens. Goat anti-mouse secondary antibodies (Thermo Fisher Scientific R37120) and NucBlue™ nuclear stain (Thermo Fisher Scientific R37605) were applied according to manufacturer recommendations. Quantification of p16 was performed using Image J to calculate the corrected total cell fluorescence of 50 cells per condition per donor. Briefly, the area of a cell is multiplied by the area integrated density of the fluorescence signal and this value is normalized to a background region near each analyzed cell. Quantification of γH2AX foci was performed using the “Find Maxima” tool in ImageJ. The number of foci were counted in approximately 100 nuclei per condition per donor. Following previous analysis strategies[28], the percentage of cells with 3 or more foci was calculated as a measure of cells with an ongoing DNA damage response.

Quantitative Polymerase Chain Reaction (qPCR)

After explant digestion, cells were plated into tissue culture plates for the purpose of subsequent RNA isolation and qPCR. After 7–12 days of monolayer culture, cells were washed with PBS and RLT buffer was directly added to lyse cells. RNA was isolated using RNeasy Mini columns (Qiagen 74104) and reverse transcription was performed using qScript XLT cDNA SuperMix (VWR International 95161). Taqman Universal Master Mix (Applied Biosystems 4304437) was used along with Taqman primer probes for the following genes: matrix metalloproteinase 13 (MMP-13, Hs00942584_m1), interleukin-6 (IL6, Hs00985639_m1), insulin-like growth factor binding protein 3 (IGFBP3, Hs00426289_m1), and C-C motif chemokine ligand 2 / monocyte chemoattractant protein 1 (CCL2, Hs00234140_m1), with TATA box binding protein (TBP, Hs00427620_m1) used as a housekeeping gene.

Histology and Chondrocyte Cluster Analysis

Human cartilage explants from 7 male and 2 female donors were fixed at the end of explant culture in 4% paraformaldehyde in PBS for 24 hours at 4°C and processed for paraffin embedding. Additionally, tissues from two sources were immediately fixed without culture: “healthy” tissue (Collins grade 0 or 1, 3 males and 3 females, average age 67.2 years) and de-identified OA waste tissue procured from total knee replacements performed at

University of North Carolina Hospitals (3 males and 4 females, average age 67.6 years). Individual donor information is provided in Figure 5C and 5E. Sections of 5 μm thickness were collected on Superfrost™ Plus slides (12-550-15; Thermo Fisher Scientific). Slides were stained with Hematoxylin (nuclei) and Eosin (cytoplasm) to detect cell cluster formation in explants. Representative bright field images were taken with an Olympus BX60 microscope. Chondrocyte cluster analysis was assessed throughout the depth of cross-sectional histological sections that began at the superficial zone and extended into the middle zone. The number of chondrocytes in singlet, doublet, and triplet or more (triplet^{+}) clusters were counted and quantified using ImageJ.

Statistical analyses

Statistical analysis and plotting were performed using Prism 8 (GraphPad, La Jolla, CA, USA) and flow cytometry data was processed with FCS Express 8 (De Novo Software, Glendale, CA, USA). Data are plotted as individual points with the mean shown. The error bars indicate the 95% confidence interval (CI) and these values are noted in parentheses on the appropriate plots. Outliers were identified using Grubbs test with $\alpha = 0.05$ and were excluded from subsequent analysis. Data from individual donors were excluded if the flow cytometry event count for any condition was less than 800 events. Outliers and excluded data are noted in the figure legends. Mean fluorescence intensity (MFI) data were normalized to the control condition for each donor to account for subtle differences in flow cytometry settings between days. Normalized MFI data in each treatment group were analyzed using a one-sample t-test against a hypothetical value of one and thus plots show a dotted line to represent this comparison. The percentage of SA-β-gal high cells was determined by introducing a cutoff at the mean plus two times the standard deviation of the control group. By Shapiro-Wilk test, these data were consistent with being sampled from a Gaussian distribution. Thus, this outcome measure was analyzed using a paired Student's t-test (equine) or Two-Way ANOVA with Tukey's Multiple Comparisons Test (human). Sample size was determined by analyzing preliminary data on three donors for the effect size and variability. It was estimated that 5–10 equine donors and 10–20 human donors would be required to detect a doubling in the main outcome measure (percentage of SA-β-gal high cells), which we determined to be biologically meaningful. With this goal, we collected as many donors as feasible in the allocated experimental timeframe. Using a post-hoc effect size calculation in SAS (POWER procedure), we determined the minimum difference that could have been detected given the actual data (sample size, mean, standard deviation) at 0.9 power and alpha = 0.05. The minimum detectable difference was 17.72 for comparison of equine explants (control vs. irradiation) and 4.11 for comparison of human explants (control 10% vs. irradiated with growth factors).

Results:

Induction of senescence in equine cartilage explants

Cartilage explants harvested from the equine stifle (patellofemoral joint) were induced to senescence in explant culture with irradiation followed by culture in monolayer for maturation of the senescent phenotype (overview of experimental design illustrated in Fig. 1). Chondrocytes from explants that had been irradiated revealed an enlarged and flattened

morphology as compared to chondrocytes from control explants (Fig. 2a). Flow cytometry for SA-β-gal activity was used to quantify the induction of senescence in the cartilage explants. A representative SA-β-gal flow plot from one equine donor is included, showing the shift in SA-β-gal fluorescence between chondrocytes cultured from the control and irradiated equine explants (Fig. 2b). The region two standard deviations above the control mean fluorescence intensity (MFI) was delineated on the SA-β-gal flow plot and was used in this study to indicate the population of SA-β-gal high cells. Chondrocytes irradiated in explant culture had significantly increased SA-β-gal activity as compared to chondrocytes from control explants (2.40-fold increase, CI 1.22 – 3.58; p = 0.027 by one-sample t-test compared to a hypothetical value of 1; Fig. 2c). The percentage of cells with high SA-β-gal activity also significantly increased in the irradiated condition as compared to control (mean difference: 21.57%, CI 14.24 – 36.54; p = 0.0031 by paired t-test; Fig. 2d). A table listing the age and sex of the equine donors is provided (Fig. 2e).

Induction of senescence in human cartilage explants

Unlike equine cartilage explants, preliminary studies indicated that irradiation alone was insufficient to induce robust senescence in human articular cartilage explants. We hypothesized that mitogenic stimulation of damaged chondrocytes would initiate the senescence phenotype and tested this by supplementing the 10% FBS media with growth factors TGF-β1 and bFGF after irradiation. Cartilage explants harvested from cadaveric human ankles of 14 donors were cultured as described for the horse explants, with the only difference being the inclusion of growth factors during explant culture as an additional variable (Fig. 1). As compared to control chondrocytes, cells digested from irradiated explants cultured with growth factors showed an enlarged morphology and the presence of bi-nucleated cells, which has been associated with senescence[29] (Fig. 3a). Experiments testing the incorporation of EdU to mark cells in S phase showed that growth factor treatment during explant culture initiated cell cycle entry that persisted in monolayer culture under control conditions (Fig. S1). A representative SA-β-gal flow cytometry plot illustrates the robust shift in SA-β-gal fluorescence with both irradiation and growth factor treatment (Fig. 3b). Chondrocytes from irradiated explants treated with TGF-β1 and bFGF showed significantly higher SA-β-gal MFI values as compared to the non-irradiated 10% FBS control (1.45 mean fold increase, CI 1.26 to 1.63; p = 0.0002 by one-sample t-test compared to a hypothetical value of 1; Fig. 3c). By this measure, chondrocytes from irradiated explants without growth factors also showed a moderate increase in SA-β-gal MFI values as compared to the non-irradiated control (1.17 mean fold increase, CI 1.03 to 1.31; p = 0.025). When the percentage of SA-β-gal high cells was analyzed by Two-way ANOVA, both irradiation and media condition, as well as the interaction, were significant factors in senescence induction. Using Tukey's multiple comparison test, the irradiated explants cultured with growth factors were significantly different than all other conditions ($p<0.005$ to all conditions) (Fig. 3d). A table listing the age and sex of the donors used in the irradiation experiments is provided (Fig. 3e).

Additional markers of the senescence phenotype

Chondrocytes isolated from explants cultured in all four conditions (control or irradiation, 10% serum media or with the inclusion of growth factors) were plated in monolayer culture

to perform additional analysis of the senescence phenotype. Analysis of γH2AX foci by immunofluorescence indicated that both irradiation and TGF-β1/bFGF treatment were required to initiate a persistent DNA damage response (Fig. 4A and B, 10.0% of cells with 3 or more foci, CI 5.0. to 15.0., all other conditions upper bound CI of ≤ 4.5.%). Quantification of p16 protein by immunofluorescence also showed the highest signal with the combination of irradiation and growth factors (Fig. 4C). The confidence interval for this group did not overlap with the confidence interval of the baseline condition (Fig. 4D, CI 13.5 to 23.2 arbitrary units per cell compared to upper bound of 10.3). Finally, qPCR analysis for 4 SASP factors was used to compare the group with the highest senescence induction (irradiation with growth factors) to the baseline control group of no irradiation with 10% serum media. This analysis showed an average fold increase of 1.29, 2.19, 1.99, and 1.68 for MMP-13, IL6, IGFBP3, and CCL2, respectively (Fig. 4E). Of these genes, IGFBP3 and CCL2 had confidence intervals with lower bounds above 1 (1.01 to 2.97 for IGFBP3 and 1.04 to 2.32 for CCL2).

Cluster formation in response to senescence-inducing conditions

H&E staining of cartilage at the end of explant culture revealed an increase in the presence of chondrocyte clusters in conditions that also resulted in senescence induction - irradiation with growth factor treatment (Fig. 5a). There was a statistically significant increase in the percentage of chondrocyte clusters in a triplet^{+} formation for the irradiation plus growth factors group as compared to all three of the other conditions ($p<0.01$, Two-way ANOVA with Tukey's multiple comparison test; Fig. 5b). The same analysis of clusters was applied to uncultured healthy cartilage (Collins grade 0 or 1) or waste OA tissue from total joint replacement. OA cartilage showed a significant increase in the percentage of clusters that are in triplet^{+} formation (28.49 with CI 20.58 to 36.4 vs. 9.69 with CI 5.39 to 13.99, $p=0.0006$ by t-test; Fig. 5d).

Discussion:

This study demonstrates that treatment of articular cartilage explants with mitogenic stimuli in the context of DNA damage reliably induces high levels of SA-β gal activity (summarized in Fig. 6). By maintaining cell-matrix interactions, this approach provides a physiologically relevant setting to investigate the initiation of senescence. Detailed characterization of the origins of cellular senescence within cartilage may provide insight into why senescent cells accumulate to pathological levels in the joint space with age and in response to joint injury. Greater understanding of senescence induction will also support the emerging therapeutic approach to target senescent cells with senolytics[30, 31], which has shown promising results in animal models for post-traumatic and age-related OA[13].

The most widely used biomarker for senescence is SA-β-gal, which distinguishes senescent cells based on high lysosomal activity[32]. Traditionally, SA-β-gal activity is detected cytochemically using 5-bromo-4-chloro-3-indolyl-β-D-galactoside (X-gal) as a substrate and by discriminating negative from positive cells by visualization of blue color in cell culture images[33]. This manual process means that only a limited number of cells can be analyzed, and the readout is subjective and binary in nature. Conversely, the SA-β-gal flow cytometry

approach utilized in this study provides a quantitative readout that captures the full range of lysosomal activity and is capable of analyzing tens of thousands of cells in a short time frame. Prior studies using a related but distinct flow cytometry readout of β-galactosidase activity revealed enhanced sensitivity as compared to the more widely used cytochemical method[33]. We also performed additional experiments to confirm that potential "false positive" signals due to confluency[34], autofluorescence[35], or the presence of dead cells did not interfere with the reported conclusion that irradiation and growth factor treatment increased true SA-β-gal activity (Fig. S2).

Full characterization of the senescent state incorporates numerous orthogonal biomarkers[36]. Thus, we assayed the extent to which three additional features of senescence are present in chondrocytes induced by the combination of DNA damage and mitogenic stimulation. First, the combination resulted in an increased number of cells with widespread γH2AX foci at the end of the monolayer culture period, indicating a persistent DNA damage response as consistent with some forms of senescence induction. Note that 10 Gy irradiation initiates a strong acute DNA damage response in chondrocytes (approximately 50% at 30–120 minutes after irradiation in monolayer culture, Fig. S3), but growth factors are required to induce a stable DNA damage response in a substantial percentage of the chondrocytes (approximately 10%). Second, we quantified the level of $p16^{INK4a}$ protein by immunofluorescence and showed that this senescence biomarker is highest in cells that are exposed to irradiation and growth factors. This is consistent with our previous finding that human chondrocytes have higher expression of $p16^{INK4a}$ with aging, although DNA damage was not explicitly measured in that study[37]. Third, we investigated whether our senescence-inducing conditions also resulted in higher SASP gene expression as compared to the control condition. While the specific components of the SASP vary based on cell type and induction stimulus, we elected to analyze expression of 4 SASP factors that are relevant to OA and had been examined in our previous work that treated murine cartilage with the same growth factor cocktail[24]. In that system, the senescence reporter allele $p16^{tdTom}$ allows for separation of senescent cells that enables a direct comparison to non-senescent cells from the same population. Results from that study showed that senescent chondrocytes have higher expression of Igfbp3, Ccl2, and Il6 (but not Mmp-13). Similarly, the current study showed an increase in IGFBP3 and CCL2, with a trend towards increased IL6 and no change in MMP-13. The observed fold increase is modest, likely because the bulk population was investigated and the SA-β-gal activity results indicate that only a subset of chondrocytes become senescent in response to the applied conditions. It is important to recognize that each of the four measures (SA-β-gal, γH2AX foci, p16 immunofluorescence, and SASP) may not score the same subset of cells as "senescent" due to varied sensitivity of the assays and the heterogeneity of senescent population[36]. However, when assessed across the population of cells derived from each culture condition, these orthogonal measures provide support for the conclusion that the mitogenic stimulation and DNA damage combine to induce senescence in human chondrocytes.

The cartilage utilized in this study originated from the equine stifle and from cadaveric human cartilage explants. The horse is a representative model of naturally occurring human osteoarthritis due to the similarities between human and equine articular cartilage and subchondral bone thickness[38]. Further, spontaneous joint injury is common in horses and

post-traumatic OA is an important challenge in veterinary care[39, 40]. In contrast to human explants, high levels of senescence were induced in equine explants without the addition of growth factors, perhaps because the cartilage from relatively young horses showed a significant mitogenic response to the serum-containing medium. It is possible that a higher dose of irradiation would be sufficient to induce senescence in human explants without growth factor stimulation, although this was not tested in the current study. The dose of 10 Gy was chosen based on the induction of senescence in other cell types[28]. Further, 10 Gy was shown to induce a level of DNA damage in porcine chondrocytes that was similar to advanced OA[41].

Cellular senescence was initially identified as an irreversible phenotype that cells entered upon reaching the limit of normal cell proliferation[42]. While chondrocytes divide in monolayer culture, this cell type is hypo-replicative when surrounded by healthy cartilage matrix *in vivo*[43], suggesting that replicative senescence is unlikely to occur at a high rate during cartilage homeostasis. However, the growth factors that are released from degrading matrix during early OA provide a potent mitogenic stimulus, as evidenced by the emergence of chondrocyte “clusters”. Increased numbers and sizes of cell clusters are characteristic of OA articular cartilage and these clusters are often localized in fissures and clefts of the upper cartilage layer[44–46]. bFGF is released from damaged cartilage tissue and has been identified near chondrocyte clusters[47]. There is also evidence of an interactive effect with TGF-β in cluster formation[48], which is of particular interest given the finding that TGF-β is a key mediator of senescence in certain contexts[49].

In this study, conditions that resulted in the highest rates of cluster formation in human explants (irradiation plus growth factors) also showed the highest rates of senescence upon maturation of the phenotype in monolayer culture. While further investigation will be required to determine the extent to which cell cycle entry plays a causal role in senescence induction, our observations that mitogenic stimulation of damaged chondrocytes induces senescence is consistent with the concept that cellular senescence arises from the coordination of two conflicting processes - cell expansion and cell-cycle arrest[20, 50, 51]. For example, studies in other quiescent and post-mitotic cell types show that the accumulation of DNA damage may not result in dysfunction until cell division is initiated[52, 53]. Our analysis of uncultured OA tissue demonstrated a similar frequency of clusters as found in explants cultured with senescence-inducing stimuli. Thus, an important area of future investigation will be to determine the extent to which cell cycle entry during OA progression initiates signaling pathways that result in subsequent senescence. One recent finding illustrates this possibility by demonstrating that Cellular Communication Network Factor 1 (CCN1, aka CYR61) increases during OA and plays a functional role in stimulating cluster formation, while inhibiting this pathway reduced the expression of senescence markers[54].

There are currently no cures for OA, and the development of effective treatments has been limited by an insufficient understanding of disease initiation and progression. This *in vitro* system establishes a set of physiological cues that induces senescence within both equine and human cartilage tissue, which will enable future mechanistic studies on senescence

induction, the role of senescent chondrocytes in cartilage dysfunction, and the use of senolytic compounds to target senescent cells as a potential treatment for OA.

Supplementary Material

Refer to Web version on PubMed Central for supplementary material.

Acknowledgements:

The authors thank Mrs. Julie Long and members of the Central Procedures Laboratory at the North Carolina State University College of Veterinary Medicine for help in isolating equine cartilage explants as well as members of Dr. Richard Loeser's laboratory at the University of North Carolina at Chapel Hill (UNC) for help in isolating human cartilage explants. The authors also would like to acknowledge the Gift of Hope Tissue and Organ Donor Bank and donor's families as well as Dr. Arkady Margulis, MD, for tissue procurement. The authors appreciate assistance from the UNC Animal Histopathology & Laboratory Medicine Core and UNC Flow Cytometry Cores, which are supported in part by a National Cancer Institute Center Core Support Grant (5P30CA016086) to the UNC Lineberger Comprehensive Cancer Center. Figures 1 and 6 of the manuscript were created using BioRender.com and exported under a paid subscription.

Role of the funding source:

None of the funding sources had a role in the study or in the decision to publish. Pilot funding was provided through a Functional Tissue Engineering Seed Grant to LVS/BOD by the Comparative Medicine Institute based at North Carolina State University (NCSU). The project described was also supported by an NC TraCS grant to BOD/LVS as part of North Carolina National Center for Advancing Translational Sciences (NCATS), National Institutes of Health, through Grant Award Number UL1TR002489. Support was also provided by a grant from the National Institute on Aging (RO1 AG044034 to RFL). The content is solely the responsibility of the authors and does not necessarily represent the official views of the NIH. Matching funds for the NC TraCS award were provided by the UNC Thurston Arthritis Research Center, the NCSU Office of Research and Innovation, and NCSU Comparative Medicine Institute. Additional support was provided by the UNC Office of the Executive Vice Chancellor and Provost through the Junior Faculty Development Award (BOD) and the Orthoregeneration Network through a Kick-Starter grant (#18-048 to BOD). Procurement of human tissue was supported in part by the Rush University Klaus Kuettner Endowed Chair for Research on Osteoarthritis (SC).

References:

1. Loeser RF, Goldring SR, Scanzello CR, Goldring MB. Osteoarthritis: a disease of the joint as an organ. Arthritis Rheum 2012; 64: 1697–1707. [PubMed: 22392533]
2. Bijlsma JW, Berenbaum F, Lafeber FP. Osteoarthritis: an update with relevance for clinical practice. Lancet 2011; 377: 2115–2126. [PubMed: 21684382]
3. Murphy L, Schwartz TA, Helmick CG, Renner JB, Tudor G, Koch G, et al. Lifetime risk of symptomatic knee osteoarthritis. Arthritis Rheum 2008; 59: 1207–1213. [PubMed: 18759314]
4. Gabriel SE, Crowson CS, Campion ME, O'Fallon WM. Direct medical costs unique to people with arthritis. J Rheumatol 1997; 24: 719–725. [PubMed: 9101508]
5. Oo WM, Yu SP, Daniel MS, Hunter DJ. Disease-modifying drugs in osteoarthritis: current understanding and future therapeutics. Expert Opin Emerg Drugs 2018; 23: 331–347. [PubMed: 30415584]
6. Kurtz SM, Ong KL, Lau E, Bozic KJ. Impact of the economic downturn on total joint replacement demand in the United States: updated projections to 2021. J Bone Joint Surg Am 2014; 96: 624–630. [PubMed: 24740658]
7. Loeser RF, Collins JA, Diekman BO. Ageing and the pathogenesis of osteoarthritis. Nat Rev Rheumatol 2016; 12: 412–420. [PubMed: 27192932]
8. Felson DT, Lawrence RC, Dieppe PA, Hirsch R, Helmick CG, Jordan JM, et al. Osteoarthritis: new insights. Part 1: the disease and its risk factors. Ann Intern Med 2000; 133: 635–646. [PubMed: 11033593]
9. Lopez-Otin C, Blasco MA, Partridge L, Serrano M, Kroemer G. The hallmarks of aging. Cell 2013; 153: 1194–1217. [PubMed: 23746838]

10. Martin JA, Buckwalter JA. Human chondrocyte senescence and osteoarthritis. Biorheology 2002; 39: 145–152. [PubMed: 12082277]
11. Price JS, Waters JG, Darrah C, Pennington C, Edwards DR, Donell ST, et al. The role of chondrocyte senescence in osteoarthritis. Aging Cell 2002; 1: 57–65. [PubMed: 12882354]
12. Rose J, Soder S, Skhirtladze C, Schmitz N, Gebhard PM, Sesselmann S, et al. DNA damage, discoordinated gene expression and cellular senescence in osteoarthritic chondrocytes. Osteoarthritis Cartilage 2012; 20: 1020–1028. [PubMed: 22659602]
13. Jeon OH, Kim C, Laberge RM, Demaria M, Rathod S, Vasserot AP, et al. Local clearance of senescent cells attenuates the development of post-traumatic osteoarthritis and creates a pro-regenerative environment. Nat Med 2017; 23: 775–781. [PubMed: 28436958]
14. Philipot D, Guerit D, Platano D, Chuchana P, Olivotto E, Espinoza F, et al. p16INK4a and its regulator miR-24 link senescence and chondrocyte terminal differentiation-associated matrix remodeling in osteoarthritis. Arthritis Res Ther 2014; 16: R58. [PubMed: 24572376]
15. Coppe JP, Desprez PY, Krtolica A, Campisi J. The senescence-associated secretory phenotype: the dark side of tumor suppression. Annu Rev Pathol 2010; 5: 99–118. [PubMed: 20078217]
16. He S, Sharpless NE. Senescence in Health and Disease. Cell 2017; 169: 1000–1011. [PubMed: 28575665]
17. Jeon OH, David N, Campisi J, Elisseeff JH. Senescent cells and osteoarthritis: a painful connection. J Clin Invest 2018; 128: 1229–1237. [PubMed: 29608139]
18. van Deursen JM. Senolytic therapies for healthy longevity. Science 2019; 364: 636–637. [PubMed: 31097655]
19. Sharpless NE, Sherr CJ. Forging a signature of in vivo senescence. Nat Rev Cancer 2015; 15: 397–408. [PubMed: 26105537]
20. Ogrodnik M, Salmonowicz H, Jurk D, Passos JF. Expansion and Cell-Cycle Arrest: Common Denominators of Cellular Senescence. Trends Biochem Sci 2019; 44: 996–1008. [PubMed: 31345557]
21. Debacq-Chainiaux F, Erusalimsky JD, Campisi J, Toussaint O. Protocols to detect senescence-associated beta-galactosidase (SA-betagal) activity, a biomarker of senescent cells in culture and in vivo. Nat Protoc 2009; 4: 1798–1806. [PubMed: 20010931]
22. Itahana K, Campisi J, Dimri GP. Methods to detect biomarkers of cellular senescence: the senescence-associated beta-galactosidase assay. Methods Mol Biol 2007; 371: 21–31. [PubMed: 17634571]
23. Liu JY, Souroullas GP, Diekman BO, Krishnamurthy J, Hall BM, Sorrentino JA, et al. Cells exhibiting strong p16 (INK4a) promoter activation in vivo display features of senescence. Proc Natl Acad Sci U S A 2019; 116: 2603–2611. [PubMed: 30683717]
24. Sessions GA, Copp ME, Liu JY, Sinkler MA, D'Costa S, Diekman BO. Controlled induction and targeted elimination of p16(INK4a)-expressing chondrocytes in cartilage explant culture. FASEB J 2019; 33: 12364–12373. [PubMed: 31408372]
25. Collins JA, Arbeeva L, Chubinskaya S, Loeser RF. Articular chondrocytes isolated from the knee and ankle joints of human tissue donors demonstrate similar redox-regulated MAP kinase and Akt signaling. Osteoarthritis Cartilage 2019; 27: 703–711. [PubMed: 30590195]
26. Muehleman C, Bareither D, Huch K, Cole AA, Kuettner KE. Prevalence of degenerative morphological changes in the joints of the lower extremity. Osteoarthritis Cartilage 1997; 5: 23–37. [PubMed: 9010876]
27. Forsyth CB, Pulai J, Loeser RF. Fibronectin fragments and blocking antibodies to alpha2beta1 and alpha5beta1 integrins stimulate mitogen-activated protein kinase signaling and increase collagenase 3 (matrix metalloproteinase 13) production by human articular chondrocytes. Arthritis Rheum 2002; 46: 2368–2376. [PubMed: 12355484]
28. Rodier F, Coppe JP, Patil CK, Hoeijmakers WA, Munoz DP, Raza SR, et al. Persistent DNA damage signalling triggers senescence-associated inflammatory cytokine secretion. Nat Cell Biol 2009; 11: 973–979. [PubMed: 19597488]
29. Leikam C, Hufnagel A, Schartl M, Meierjohann S. Oncogene activation in melanocytes links reactive oxygen to multinucleated phenotype and senescence. Oncogene 2008; 27: 7070–7082. [PubMed: 18806824]

30. Munoz-Espin D, Serrano M. Cellular senescence: from physiology to pathology. Nat Rev Mol Cell Biol 2014; 15: 482–496. [PubMed: 24954210]
31. Xu M, Pirtskhalava T, Farr JN, Weigand BM, Palmer AK, Weivoda MM, et al. Senolytics improve physical function and increase lifespan in old age. Nat Med 2018; 24: 1246–1256. [PubMed: 29988130]
32. Lee BY, Han JA, Im JS, Morrone A, Johung K, Goodwin EC, et al. Senescence-associated beta-galactosidase is lysosomal beta-galactosidase. Aging Cell 2006; 5: 187–195. [PubMed: 16626397]
33. Noppe G, Dekker P, de Koning-Treurniet C, Blom J, van Heemst D, Dirks RW, et al. Rapid flow cytometric method for measuring senescence associated beta-galactosidase activity in human fibroblasts. Cytometry A 2009; 75: 910–916. [PubMed: 19777541]
34. Yang NC, Hu ML. The limitations and validities of senescence associated-beta-galactosidase activity as an aging marker for human foreskin fibroblast Hs68 cells. Exp Gerontol 2005; 40: 813–819. [PubMed: 16154306]
35. Bertolo A, Baur M, Guerrero J, Potzel T, Stoyanov J. Autofluorescence is a Reliable in vitro Marker of Cellular Senescence in Human Mesenchymal Stromal Cells. Sci Rep 2019; 9: 2074. [PubMed: 30765770]
36. Gorgoulis V, Adams PD, Alimonti A, Bennett DC, Bischof O, Bishop C, et al. Cellular Senescence: Defining a Path Forward. Cell 2019; 179: 813–827. [PubMed: 31675495]
37. Diekman BO, Sessions GA, Collins JA, Knecht AK, Strum SL, Mitin NK, et al. Expression of p16(INK)(4a) is a biomarker of chondrocyte aging but does not cause osteoarthritis. Aging Cell 2018: e12771. [PubMed: 29744983]
38. McIlwraith CW, Frisbie DD, Kawcak CE. The horse as a model of naturally occurring osteoarthritis. Bone Joint Res 2012; 1: 297–309. [PubMed: 23610661]
39. McIlwraith CW, Fortier LA, Frisbie DD, Nixon AJ. Equine Models of Articular Cartilage Repair. Cartilage 2011; 2: 317–326. [PubMed: 26069590]
40. Goodrich LR, Nixon AJ. Medical treatment of osteoarthritis in the horse - a review. Vet J 2006; 171: 51–69. [PubMed: 16427582]
41. Chen AF, Davies CM, De Lin M, Fermor B. Oxidative DNA damage in osteoarthritic porcine articular cartilage. J Cell Physiol 2008; 217: 828–833. [PubMed: 18720406]
42. Hayflick L, Moorhead PS. The serial cultivation of human diploid cell strains. Exp Cell Res 1961; 25: 585–621. [PubMed: 13905658]
43. Aigner T, Hemmel M, Neureiter D, Gebhard PM, Zeiler G, Kirchner T, et al. Apoptotic cell death is not a widespread phenomenon in normal aging and osteoarthritis human articular knee cartilage: a study of proliferation, programmed cell death (apoptosis), and viability of chondrocytes in normal and osteoarthritic human knee cartilage. Arthritis Rheum 2001; 44: 1304–1312. [PubMed: 11407689]
44. Lotz MK, Otsuki S, Grogan SP, Sah R, Terkeltaub R, D'Lima D. Cartilage cell clusters. Arthritis Rheum 2010; 62: 2206–2218. [PubMed: 20506158]
45. Lee GM, Paul TA, Slabaugh M, Kelley SS. The incidence of enlarged chondrons in normal and osteoarthritic human cartilage and their relative matrix density. Osteoarthritis Cartilage 2000; 8: 44–52. [PubMed: 10607498]
46. Mankin HJ, Dorfman H, Lippiello L, Zarins A. Biochemical and metabolic abnormalities in articular cartilage from osteo-arthritic human hips. II. Correlation of morphology with biochemical and metabolic data. J Bone Joint Surg Am 1971; 53: 523–537. [PubMed: 5580011]
47. Vincent T, Hermansson M, Bolton M, Wait R, Saklatvala J. Basic FGF mediates an immediate response of articular cartilage to mechanical injury. Proc Natl Acad Sci U S A 2002; 99: 8259–8264. [PubMed: 12034879]
48. Quintavalla J, Kumar C, Daouti S, Slosberg E, Uziel-Fusi S. Chondrocyte cluster formation in agarose cultures as a functional assay to identify genes expressed in osteoarthritis. J Cell Physiol 2005; 204: 560–566. [PubMed: 15799031]
49. Acosta JC, Banito A, Wuestefeld T, Georgilis A, Janich P, Morton JP, et al. A complex secretory program orchestrated by the inflammasome controls paracrine senescence. Nat Cell Biol 2013; 15: 978–990. [PubMed: 23770676]

50. Blagosklonny MV. Geroconversion: irreversible step to cellular senescence. Cell Cycle 2014; 13: 3628–3635. [PubMed: 25483060]

51. Serrano M, Lin AW, McCurrach ME, Beach D, Lowe SW. Oncogenic ras provokes premature cell senescence associated with accumulation of p53 and p16INK4a. Cell 1997; 88: 593–602. [PubMed: 9054499]

52. Flach J, Bakker ST, Mohrin M, Conroy PC, Pietras EM, Reynaud D, et al. Replication stress is a potent driver of functional decline in ageing haematopoietic stem cells. Nature 2014; 512: 198–202. [PubMed: 25079315]

53. Sousa-Victor P, Gutarra S, Garcia-Prat L, Rodriguez-Ubreva J, Ortet L, Ruiz-Bonilla V, et al. Geriatric muscle stem cells switch reversible quiescence into senescence. Nature 2014; 506: 316–321. [PubMed: 24522534]

54. Feng M, Peng H, Yao R, Zhang Z, Mao G, Yu H, et al. Inhibition of cellular communication network factor 1 (CCN1)-driven senescence slows down cartilage inflammaging and osteoarthritis. Bone 2020; 139: 115522. [PubMed: 32622876]

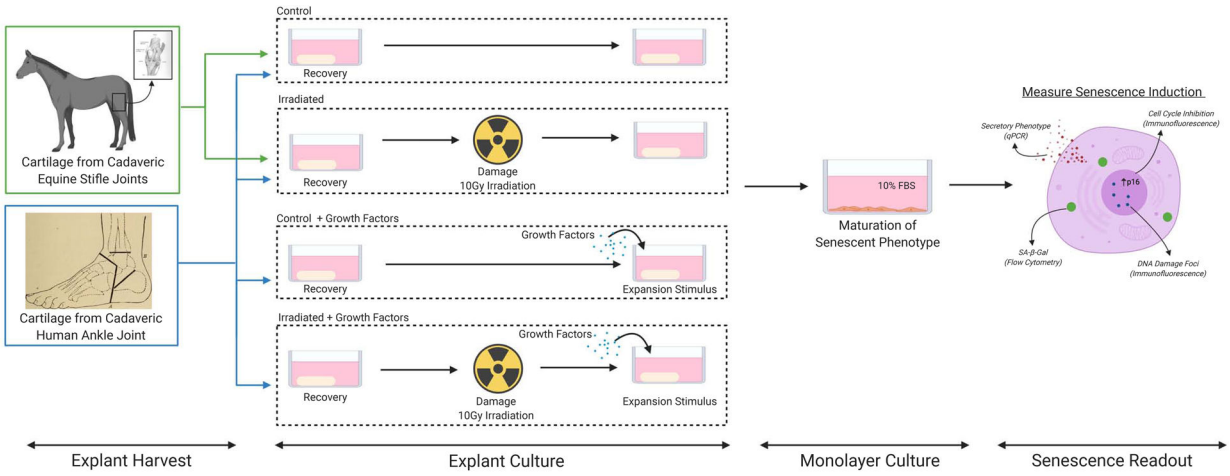

Figure 1. Experimental system schematic.

Senescence was induced in healthy cadaveric cartilage by damaging explants with irradiation (10 Gy), culturing the explants for 7 to 10 days, followed by enzymatic digestion and culture in monolayer for an additional 10 to 12 days. For human explants the effect of adding the growth factors TGF-β1 and bFGF was investigated. Senescence induction was assessed via SA-β-gal flow cytometry, qPCR, and immunofluorescence. Figure Created with BioRender.com.

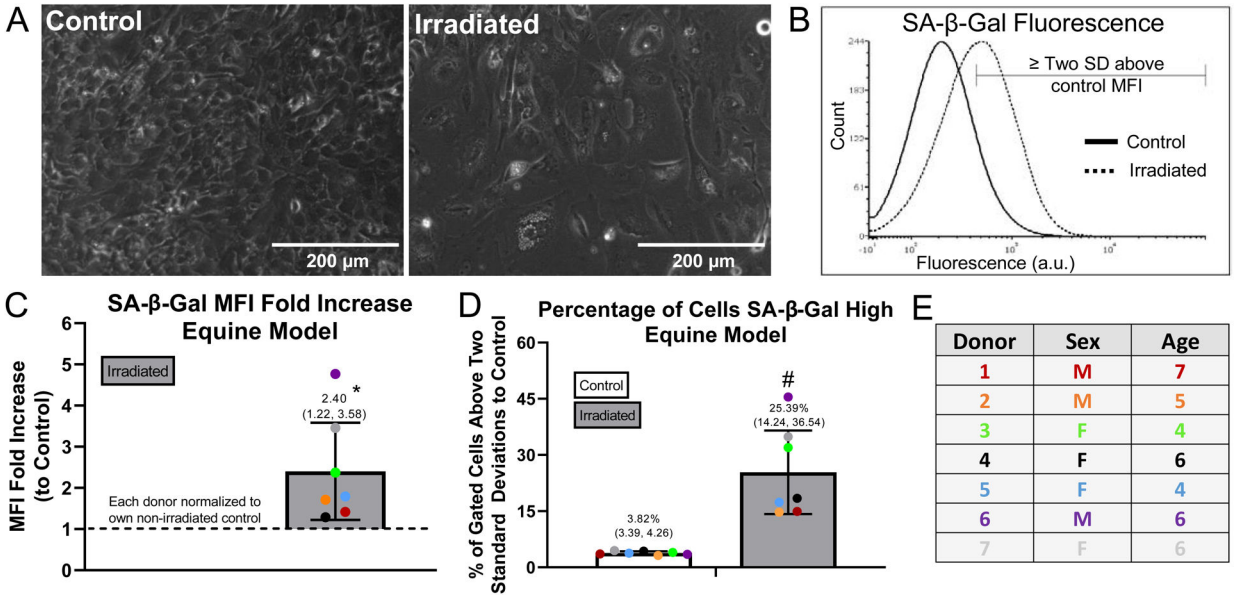

Donor	Sex	Age
1	M	7
2	M	5
3	F	4
4	F	6
5	F	4
6	M	6
7	F	6

Figure 2. Quantification of senescence induction within equine explants.

Equine explants were divided into control and irradiated groups, cultured in explant form for 7 to 10 days, digested, and cultured in monolayer for an additional 10 to 12 days in 10% FBS for maturation of the senescence phenotype. (A) Morphology of control and irradiated chondrocytes from Equine Donor 3 after 12 days of monolayer culture; scale bar = 200 µm. (B) Representative SA-β-Gal flow cytometry plot with the region two standard deviations above control MFI marked (Equine Donor 3). (C) SA-β-Gal mean fluorescence intensity (MFI) fold increase above control quantified; (*) indicates significance by one-sample t-test compared to a hypothetical value of 1, p=0.0272. (D) SA-β-Gal flow quantified as percentage of cells SA-β-Gal high. SA-β-Gal high cells delineated as those expressing SA-β-Gal fluorescence above 2 standard deviations from the control MFI; (#) indicates significance by paired t-test, p=0.0031. (E) Information from equine donors included in the analysis (n=7 thoroughbred horses), no horses excluded from analysis.

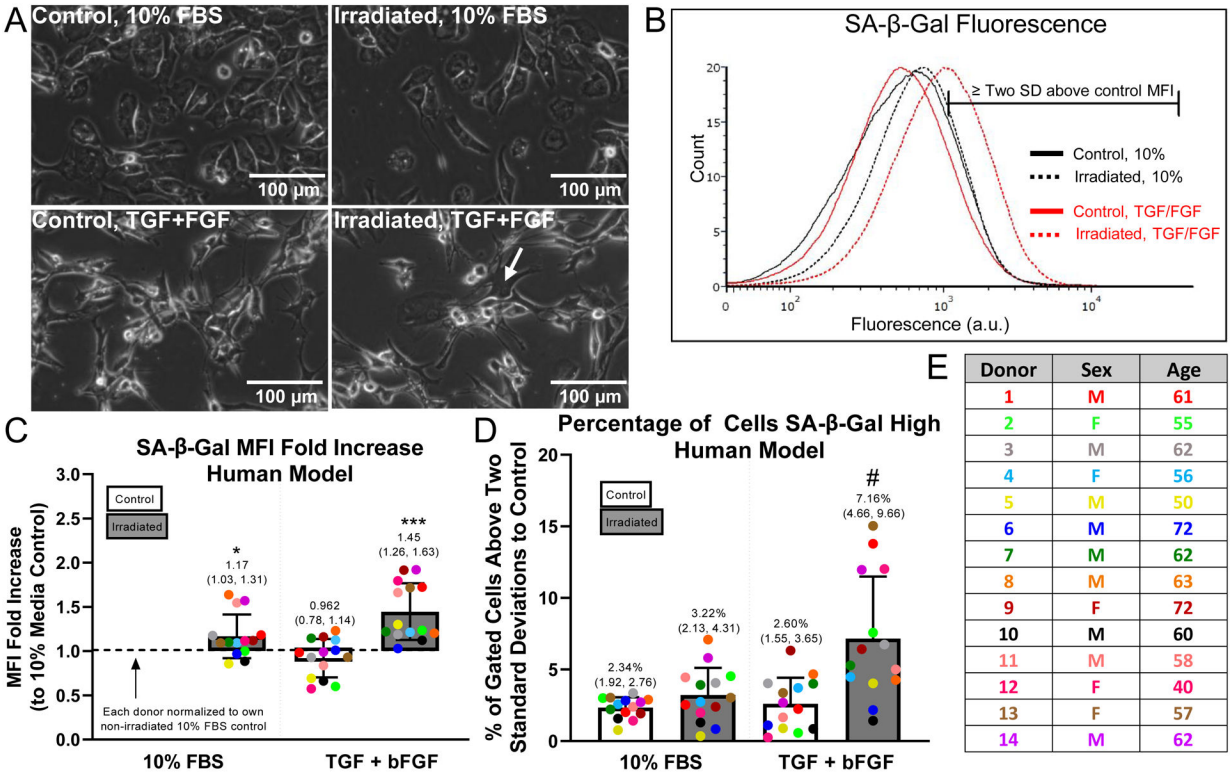

E

Donor	Sex	Age
1	M	61
2	F	55
3	M	62
4	F	56
5	M	50
6	M	72
7	M	62
8	M	63
9	F	72
10	M	60
11	M	58
12	F	40
13	F	57
14	M	62

Figure 3. Quantification of senescence induction within human explants.

Human explants were divided into control and irradiated groups, cultured in explant form for 7 days, then cultured in monolayer for an additional 12 days in 10% FBS for maturation of senescence phenotype. Growth factors, 1 ng/mL TGF-β1 and 5 ng/mL bFGF, were added to the 10% FBS in the explant culture to provide a mitogenic stimulus. (A) Morphology of chondrocytes digested from control or irradiated cartilage (treated with or without growth factors) after 12 days of monolayer culture in 10% FBS medium (Human Donor 14); scale bar = 100 µm; arrow indicates bi-nucleated cell. (B) Representative SA-β-Gal flow cytometry plot with the region two standard deviations above control MFI marked (Human Donor 1). (C) SA-β-Gal MFI fold increase above the control 10% condition quantified; (*) indicates significance by one-sample t-test compared to a hypothetical value of 1, p=0.025; (***) indicates significance by one-sample t-test compared to a hypothetical value of 1, p=0.0002. (D) SA-β-Gal flow quantified as the percentage of cells SA-β-Gal high; (#) indicates significance to all other groups by 2-way ANOVA with Tukey's multiple comparison test, p<0.005. (E) Information from human cartilage donors included in the analysis (n=14); three donors excluded due to too few cells (<800 events) in SA-β gal flow cytometry experiment and one outlier identified by Grubbs test and removed from subsequent analysis.

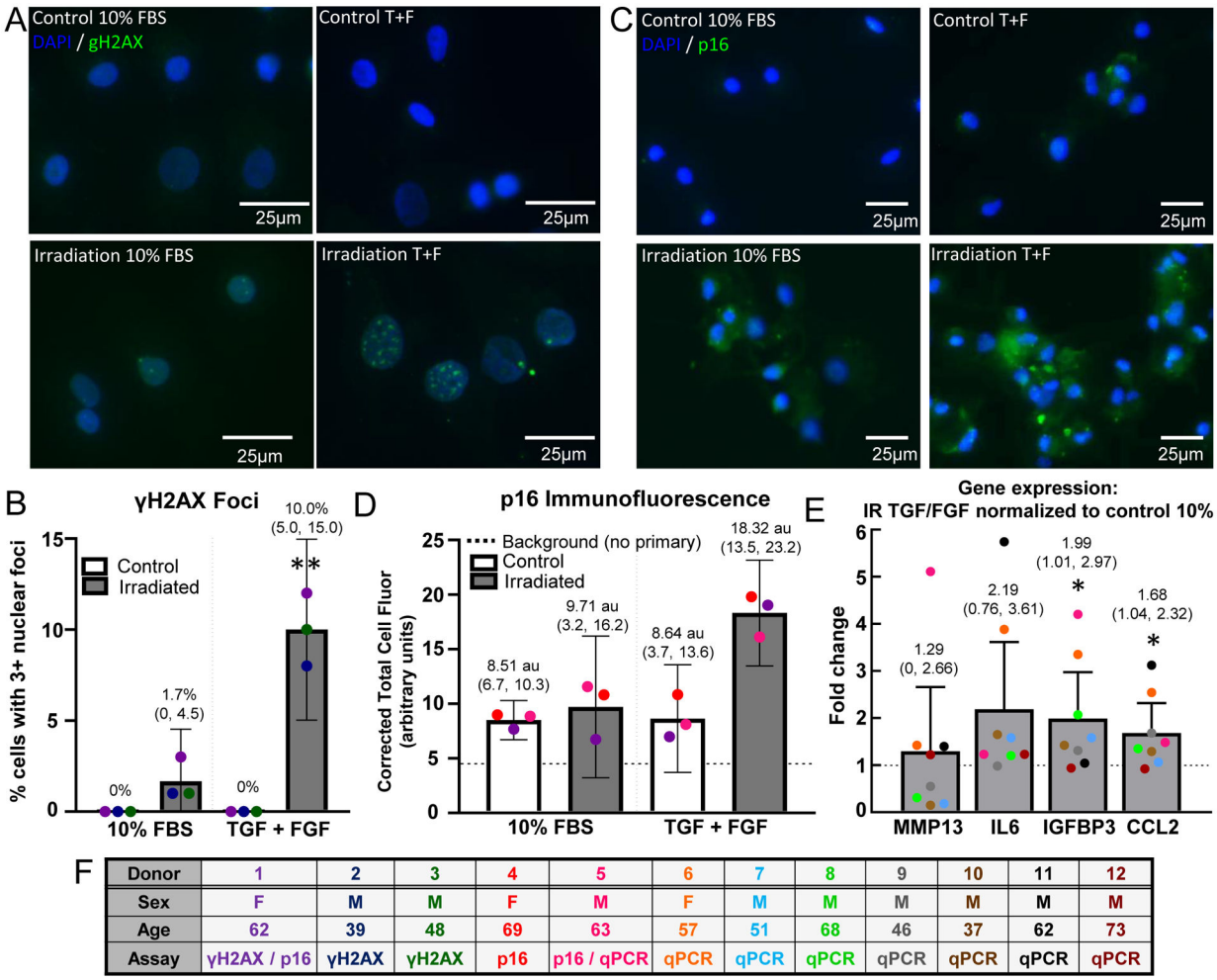

F

Donor	1	2	3	4	5	6	7	8	9	10	11	12
Sex	F	M	M	F	M	F	M	M	M	M	M	M
Age	62	39	48	69	63	57	51	68	46	37	62	73
Assay	γH2AX / p16	γH2AX	γH2AX	p16	p16 / qPCR	qPCR	qPCR	qPCR	qPCR	qPCR	qPCR	qPCR

Figure 4. Verification of senescence induction.

Control and irradiated explants were either treated with 10% FBS or 10% FBS spiked with TGF and bFGF, then digested and plated in monolayer. (A) γH2AX immunofluorescence was used to identify sustained DNA damage; scale bar = 25 μm. (B) The γH2AX images were analyzed by quantifying the number of nuclei with three or more γH2AX puncta; (**) indicates significance to all other groups by 2-way ANOVA with Tukey's multiple comparison test, $p<0.005$ (n=3) (C) p16 immunofluorescent images at the end of monolayer culture for each condition. (D) The p16 corrected total cell fluorescence normalized to cell area was quantified for each condition. The irradiation + TGF/FGF treated cells had a higher total cell fluorescence compared to the other groups (n=3). (E) qPCR was performed to measure the SASP expression from the chondrocytes at the end of monolayer culture. The fold change in gene expression in the irradiation + TGF/FGF group to the control group for MMP13, IL-6, IGFBP3, and CCL2 is plotted; (*) indicates significance by one-sample t-test compared to a hypothetical value of 1, $p<0.05$. (F) Human donor information. Note that donor numbering and color coding do not match Figure 3.

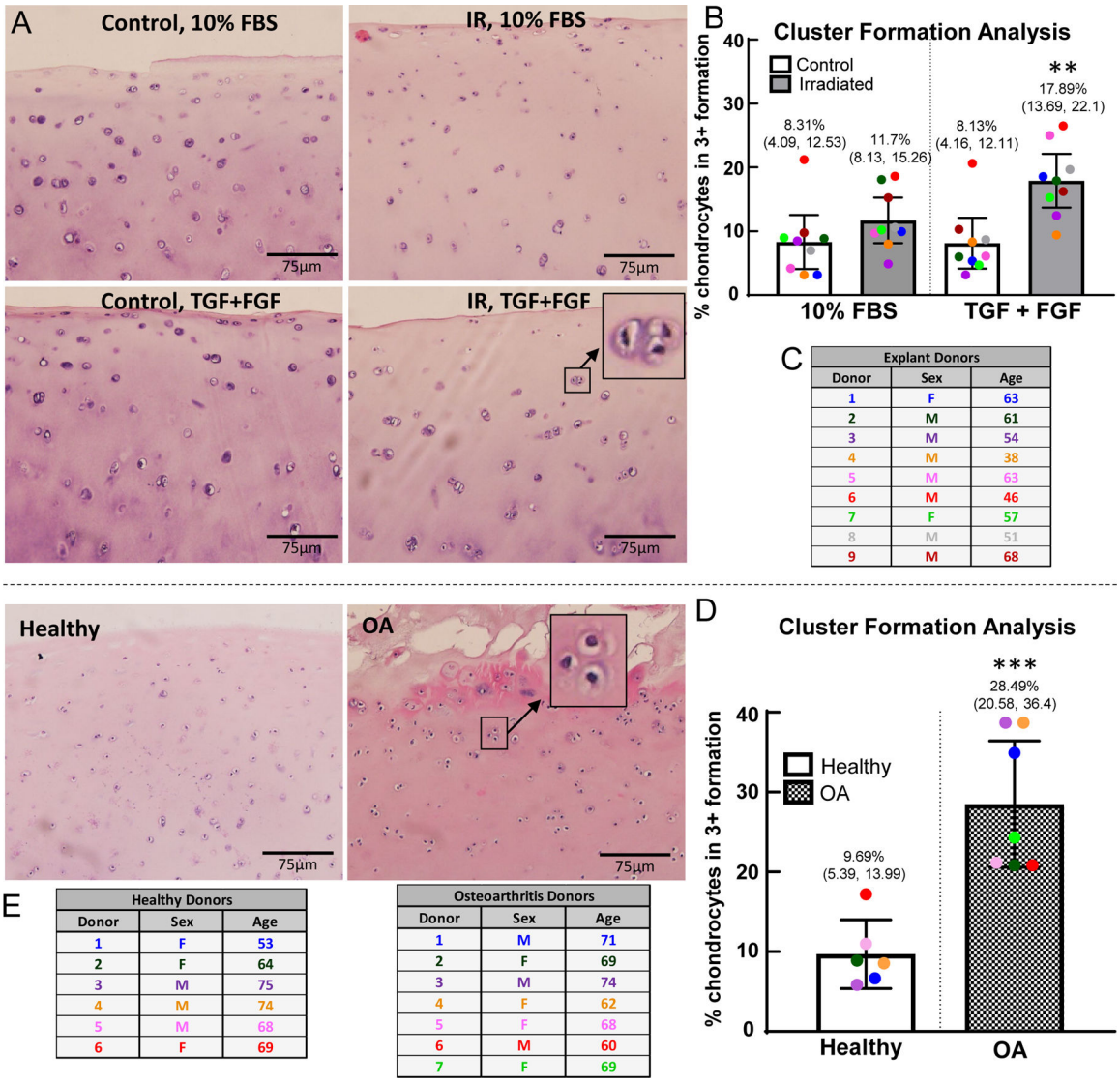

Figure 5. Chondrocyte clusters in cartilage explants.

The chondrocyte clusters in the superficial and middle zones for the control and experimental conditions were analyzed using ImageJ. (A) H&E staining on control and irradiated explants after explant culture for 7 days, with or without growth factors (Explant Donor 7). H&E staining of healthy and osteoarthritic cartilage (Healthy Donor 4, OA Donor 7). (B) Cell cluster analysis on cultured explants, with percentage of all clusters (including individual cells as a cluster) in triplet^{+} formation; (**) indicates significance by 2-way ANOVA with Tukey's multiple comparison test to all other groups, $p<0.01$ (C) Table of the human cartilage donors included in the analysis, (n=9). One outlier identified by Grubb's test and removed from analysis. (D) Cell cluster analysis on healthy and OA cartilage; (***) indicates significance by unpaired t-test, $p=0.0006$ (E) Table of the human osteoarthritis cartilage donors and healthy cartilage donors included in the analysis (n=6 healthy donors, n=7 OA donors). Average age of healthy donors is 67.2 years (3 males, 3 females); average age of OA donors is 67.6 years (3 males, 4 females). No outliers removed from analysis.

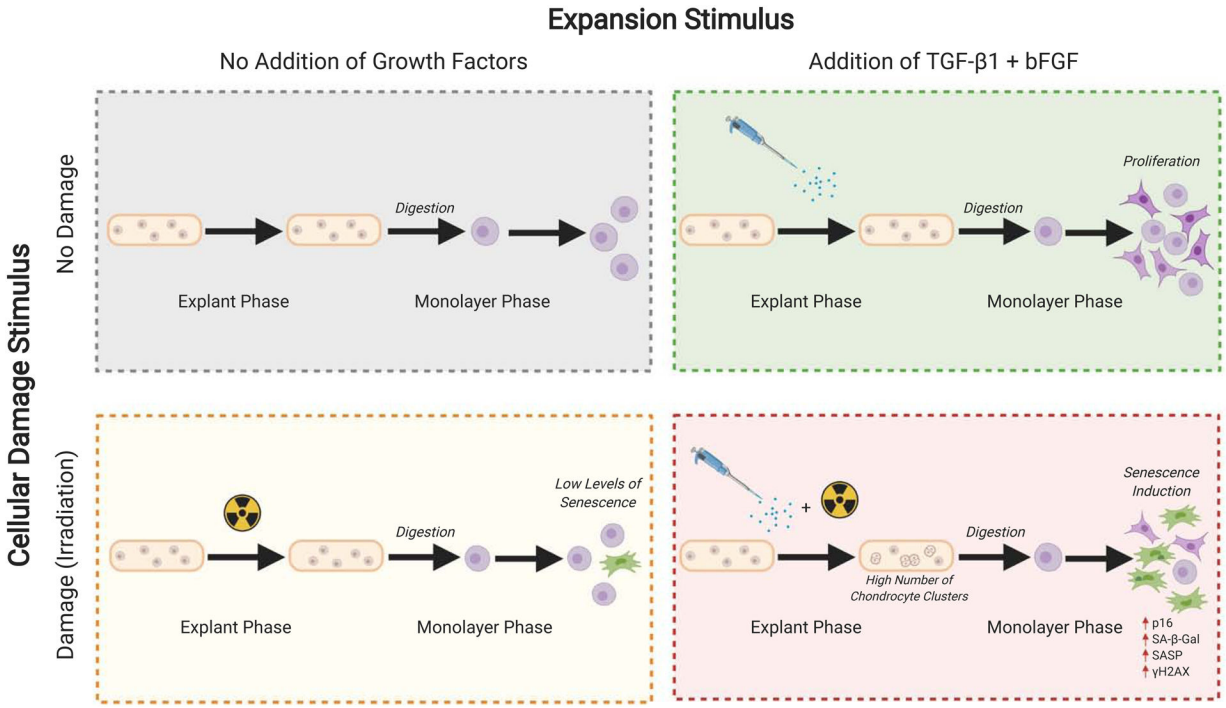

Figure 6. Overview of the senescence induction process.

The senescence induction phenotype is hypothesized to be a result of conflicting cues from cellular damage stimuli and expansion stimuli. In the context of this study, the expansion stimulus was provided by 10% FBS (equine model) and 10% FBS + bFGF + TGF-β1 (human model), while the cellular damage stimulus was provided by 10 Gy of irradiation. Figure created with BioRender.com.